

111
9 AFGL-TR-76-0097, AFGL-AFSG-342
AIR FORCE SURVEYS IN GEOPHYSICS NO. 342

12
B.S.

ADA 026509

6 Ionospheric Scintillation Effects on VHF-UHF Communication Systems.

10 HERBERT E. WHITNEY

11 3 May 1976

12 23 p.

16 AF-4643

D D C
JUL 7 1976
A 87

Approved for public release; distribution unlimited.

17 4643 QL

IONOSPHERIC PHYSICS DIVISION PROJECT 4643
AIR FORCE GEOPHYSICS LABORATORY
HANSCOM AFB, MASSACHUSETTS 01731

AIR FORCE SYSTEMS COMMAND, USAF



409 578 AB

This technical report has been reviewed and
is approved for publication.

AFGL-TR-76-0097 *AD 006509*
AIR FORCE SURVEYS IN GEOPHYSICS, NO. 342
3 MAY 1976

IONOSPHERIC SCINTILLATION EFFECTS ON VHF-UHF
COMMUNICATION SYSTEMS

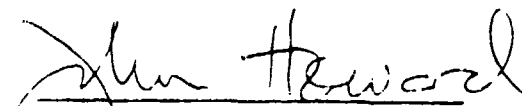
Herbert E. Whitney

Errata

Place this notice inside of the front cover:

This technical report has been reviewed and
is approved for publication.

FOR THE COMMANDER:



Chief Scientist

Qualified requestors may obtain additional copies from the Defense
Documentation Center. All others should apply to the National
Technical Information Service.

AIR FORCE GEOPHYSICS LABORATORY
AIR FORCE SYSTEMS COMMAND
UNITED STATES AIR FORCE
HANSCOM AFB, MASSACHUSETTS 01731

Unclassified

SECURITY CLASSIFICATION OF THIS PAGE(When Data Entered)

20. (Cont)

scintillations in the 225 to 400 MHz band. The rate of scintillation is described by level crossing techniques, power spectra, and correlation functions. The effectiveness of diversity techniques is indicated. The spectral index was measured as approximately (-0.2) , indicating that intense scintillations can become almost frequency independent in this range.

f to the minus 0.2 power,

ACCESSION NO.	
NTIS	
DDO	
WHO	
JUL	
BY...	
DATE	
A	

Unclassified

SECURITY CLASSIFICATION OF THIS PAGE(When Data Entered)

Contents

1. INTRODUCTION	5
2. DATA - FORMAT AND ANALYSIS	6
3. RESULTS	15
4. CONCLUSIONS AND RECOMMENDATIONS	20
REFERENCES	21

Illustrations

1. Chart Record of Scintillations and Resulting Cumulative Amplitude Distributions for 137 MHz and 360 MHz ATS-6 Signals Received at Huancayo, Peru. The measured m values are 1.1 for the 137 MHz distribution and 1.7 for the 360 MHz distribution	8
2. Cumulative Distributions of the Duration of the Scintillations Shown in Figure 1	8
3. Effect of Scintillations on the Ability to Receive Perfect Messages of Various Lengths	9
4. Typical Power Spectra for Intense Scintillations at 137 MHz and 360 MHz	11
5. Typical Autocorrelation Functions for Intense Scintillations at 137 MHz and 360 MHz	13
6. Typical Crosscorrelation Data for Intense Scintillations at 137 MHz and 360 MHz	14

Illustrations

7.	Cumulative Form of Nakagami m -Distribution; Valid for $m \geq 0.5$	16
8.	Occurrence of Spectral Index (η_m) Values From a Data Base of 17 Pair of 15-min Amplitude Distribution of 137 and 360 MHz Scintillations, m = Nakagami's Distribution Parameter	17
9.	Improvement in Signal-to-Noise Ratio With Dual-Diversity Techniques Under Conditions of Rayleigh Fading	18
10.	Variation of Autocorrelation Intervals for Two Frequency Data Samples	18
11.	Variation of the Correlation Interval With Intensity of Scintillations for Two Frequency Data Samples	19

Tables

1.	Summary of Data Base	6
2.	Summary of Data Reduction	12

Ionospheric Scintillation Effects on VHF-UHF Communication Systems

1. INTRODUCTION

Satellite communication links at UHF can be subject to the effects of ionospheric scintillations, which are principally related to the occurrence of F-layer irregularities. Scintillations cause both enhancements and fading about the median level as the radio signal transits the disturbed ionospheric region. When scintillations occur which exceed the fade margin, performance of the communications link will be degraded. This degradation is most serious for propagation paths which transit the auroral and equatorial ionospheres. The degree of degradation will depend on how far the signal fades below the margin, the duration of the fade, the type of modulation and the criteria for acceptability.

The occurrence of scintillations has been studied for several years and its morphology has been documented for the auroral, mid-latitude and equatorial regions.^{1, 2, 3} This report concentrates on the analysis of specific periods of intense scintillations and applies the results to the evaluation of communication system performance.

(Received for publication 3 May 1976)

1. Aarons, J., Whitney, H. E., and Allen, R. S. (1971) Global morphology of ionospheric scintillations, Proc. IEEE 59:159.
2. Crane, R. K. (1974) Morphology of Ionospheric Scintillation, Technical Note. Lincoln Laboratory, 1974-29, Air Force Contract F19628-73-C-0002.
3. Aarons, J. (1975) Global Morphology of Ionospheric Scintillations II, AFCRL-TR-75-0135.

2. DATA -- FORMAT AND ANALYSIS

Data from Huancayo, Peru and Narssarssuaq, Greenland were used for this study. The data were analyzed in 15-min intervals as earlier studies⁴ had shown that this length was a good choice for scintillation studies using synchronous satellites. The periods covered by each set of data are listed in Table 1.

Table 1. Summary of Data Base

Site	Freq (MHz)	Date	Time (UT)	No. of 15-min. Intervals
Peru	137/360	2 Nov 1974	0315 to 0500	7
Peru	137/360	5 Nov 1974	0118 to 0433	10
Narssarssuaq	137	20 Jul 1974	0500 to 0830	14

This selection of data provided a total of 31 periods of quite intense scintillations. These data were not selected to represent 'worst' case conditions but only a sampling of strong scintillations that can occur in the polar, auroral and equatorial regions. The 360 MHz data from Peru was at a frequency of direct interest to AFSATCOM, while only 137 MHz data was available on magnetic tape from Narssarssuaq. The Peru data was emphasized because it exhibited the strongest scintillation and had two frequencies which provided a measure of the spectral index or frequency dependence of scintillation for this frequency range.

The signal strength level from satellite beacons was recorded on FM analog tape and then digitized at six samples per sec for computer processing. A relative calibration of the complete receiving and recording equipment was accomplished near the time of each scintillation record.

A computer program was written that provided the following outputs:

- (a) IBM plot of the signal level,
- (b) cumulative probability amplitude distribution, cdf,
- (c) fade rate distributions,
- (d) message reliability,
- (e) power spectrum,
- (f) autocorrelation, and
- (g) cross-correlation.

4. Whitney, H. E., Aarons, J., Allen, R. S., and Seemann, D. R. (1972) Estimation of the cumulative amplitude probability distribution function of ionospheric scintillations, Radio Science, 7, No. 12:1095-1104.

An example of each of the outputs is shown in Figures 1 through 6 for both the 137 MHz and 360 MHz data.

A 15-min section of the chart recording at each frequency and the resulting cdf is shown in Figure 1. The cdf is a first order statistic and is useful for defining the minimum margin requirements for the communications link of nondiversity systems. The various scintillation indices defined by Briggs and Parkins,⁵ that is, S_1 , S_2 , S_3 and S_4 are calculated for each 15-min sample. S_4 which depends on the rms value of the power, is the most commonly used index. The Nakagami m-distribution⁶ has been shown⁴ to be practically useful for describing the effects of scintillations on satellite communication links. Christopher⁷ has described a useful application of the moments of a log-Nakagami distribution. Also calculated for each 15-min interval are the Nakagami m-value, ($m = 1/S_4^2$); a Chi-square fitness test of the experimental data to both Nakagami and log-normal distributions over the 2 to 98 percentile range; and the first four moments, MU, of the log-Nakagami pdf. The circles in Figure 1 are points for a Rayleigh distribution ($m = 1$) and show the agreement with the experimental data.

In addition to the information on the amplitude of the fades which is given by the cdf, statistical descriptions of the fading rate is needed in order to fully characterize the effects of scintillations on the communications channel. Information on the fading rate can either be produced by level-crossing techniques or by Fourier techniques which produce the power spectra and time correlation functions. The level-crossing data give measurements of the distribution of the fades and enhancements at various levels relative to the median level. The duration and separation of the fades are counted and tabulated against time intervals for 1 dB changes in signal level down to -10 dB. Intervals shorter than 0.25 sec and longer than 60 sec were not resolved. Figure 2 shows the distribution of fades below several levels for both 137 MHz and 360 MHz. For this particular sample the occurrence of fades of a given duration at 137 MHz was approximately twice that occurring at 360 MHz. The presentation of enhancements of signals for various levels can be done in a similar manner.

Figure 3 shows a plot of the message reliability for both frequencies. This given an estimate of the increase in margin which is required over the value specified by the cdf to obtain a given probability of receiving perfect messages. Message reliability was measured by determining the number of time intervals or messages

5. Briggs, B.H., and Parkins, I.A. (1963) On the variation of radio star and satellite scintillations with zenith angle, J. Atmos. Terr. Phy., 25:330.366.
6. Nakagami, M. (1960) Statistical methods in Radio Wave Propagation, edited by W.C. Hoffman, pp. 3-36, Pergamon, New York
7. Christopher, P. (1975) Moments of a Log-Nakagami Distribution and Application, Mitre Corporation Memo D91-M-4024.

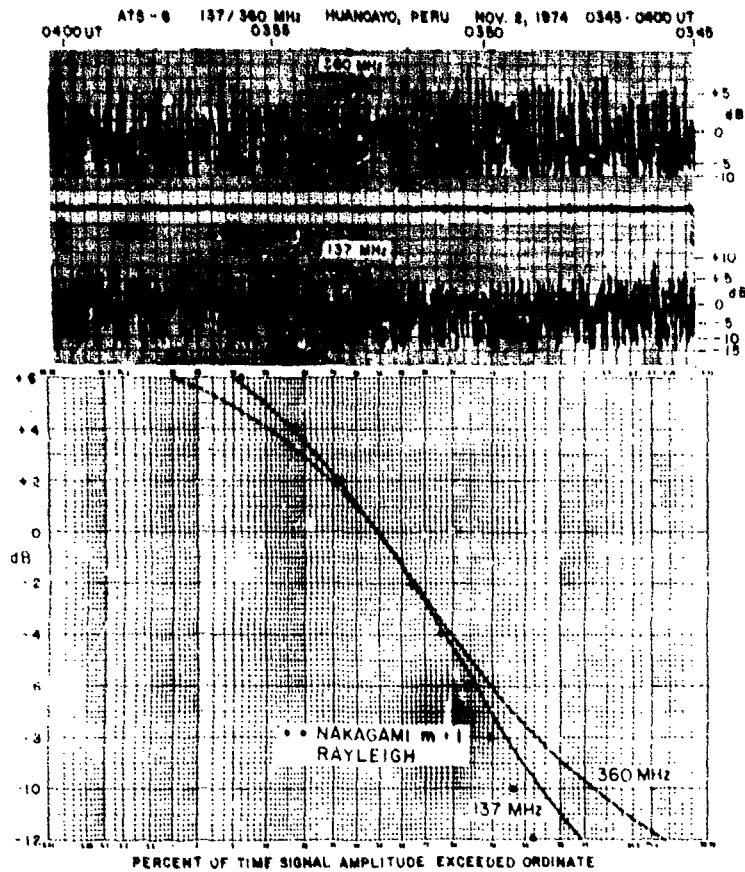


Figure 1. Chart Record of Scintillations and Resulting Cumulative Amplitude Distributions for 137 MHz and 360 MHz ATS-6 Signals Received at Huancayo, Peru. The measured m values are 1.1 for the 137 MHz distribution and 1.7 for the 360 MHz distribution

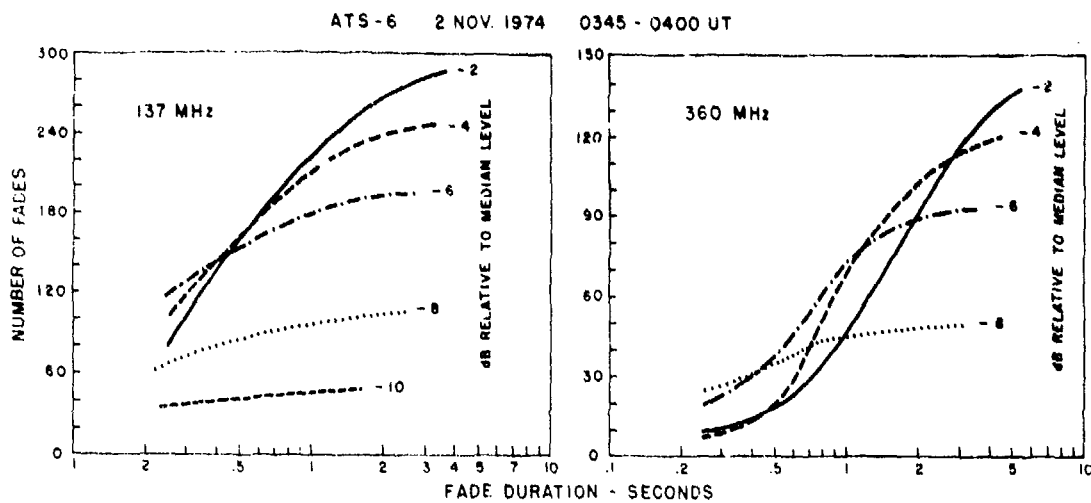


Figure 2. Cumulative Distributions of the Duration of the Scintillations Shown in Figure 1

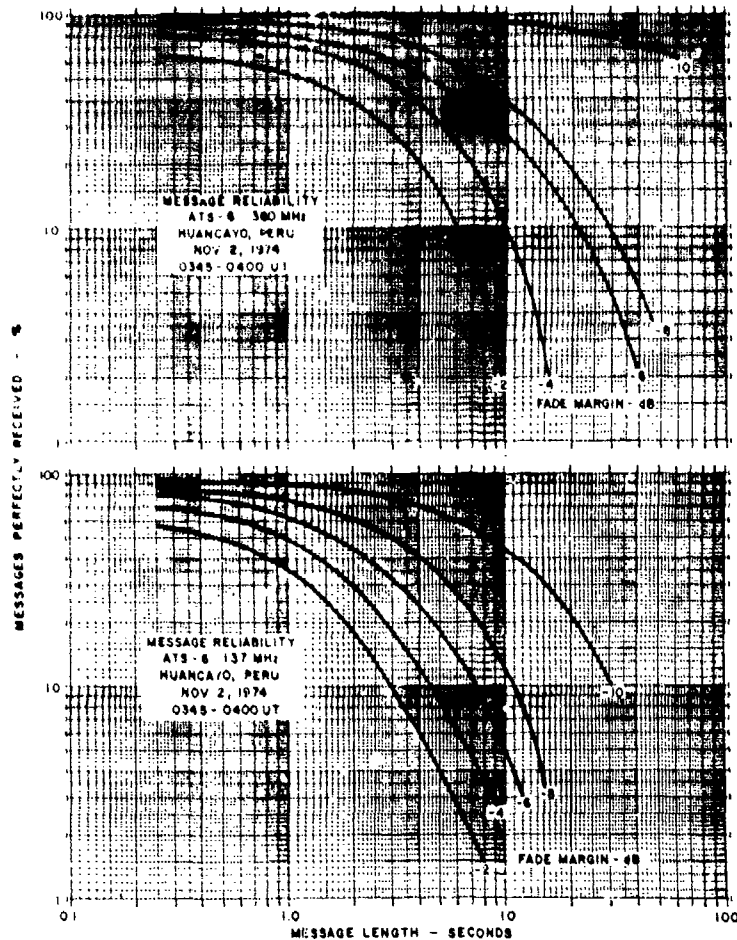


Figure 3. Effect of Scintillations on the Ability to Receive Perfect Messages of Various Lengths

that completely fit within the signal enhancements or increases above specified calibration levels compared with the total possible number in a 15-min period. Since the calibration levels are relative to the median level they can represent various values of the fade margin. The data sample is long (15 min) compared with typical message lengths. Therefore changing the time of synchronization results in only a minor variation to the calculated value of message reliability. As the time interval (message length) approaches zero the message reliability approaches the percentile given by the cdf at that fade level. Therefore the cdf gives the maximum possible value of message reliability. The curves show message reliability approaches zero as the message length increases. For example, for a four-sec message length, approximately 40 percent of the messages would be perfectly received at the -8 dB fade margin level at 137 MHz and 70 percent at 360 MHz. As

the fading rate increases the curves will fall off more rapidly. If the fading rate becomes so rapid that the inter-fade separations are less than the message length, no messages will be received without error.

Figure 4 shows the 137 MHz and 360 MHz power spectra for this data sample. The rate of the scintillation fading is characterized by the power spectrum. In general, the spectral shape consists of a relatively flat low frequency spectrum and a high frequency roll-off with a slope of approximately f^{-5} for intense scintillations. A 'cut-off' frequency denotes the break point between the low and high frequency slopes. Some spectra had a fairly abrupt transition in the 0.1 to 1 Hz range between the low and high frequency bands and the intersection of straight line fits to the slopes give the 'cut-off' frequency. The results are tabulated in Table 2. Other spectra did not exhibit a 'cut-off' frequency and only a single slope was measured. The strong discrete lines are associated with the satellite spin modulation.

Figure 5 shows the 137 MHz and 360 MHz autocorrelation functions for the data sample. The autocorrelation function is another way of characterizing the rate of scintillation fading. It is the Fourier transform of the power spectrum and therefore has a width which is inversely proportional to the bandwidth of the power spectrum where the bandwidth is defined by the 'cut-off' frequency. The correlation interval, τ is necessary to evaluate the effectiveness of time diversity. Coding techniques can be an effective means of achieving time diversity improvement. The correlation for the full period is plotted and in addition the first 16 sec is expanded. The correlation interval, τ , is printed out for coefficients of approximately 0.5, 0 and at the first inflection point.

Figure 6 shows the cross-correlation function of the 137 MHz and 360 MHz channels. It indicates the effectiveness of applying frequency diversity techniques to overcome the degradation due to scintillations. The cross-correlation coefficient was less than 0.2 for this sample and also was low ($<.4$) for two other data samples that were analyzed. It is expected that the cross-correlation values would be low for this wide a frequency difference (137/360 MHz) under conditions of intense scintillations. Since Schwartz et al⁸ indicates only a very small improvement in diversity gain for correlation coefficients between 0.5 and 0 the computation of the cross-correlation function was not done for all the two frequency data. From the standpoint of the needs of the AFSATCOM program it would have been more desirable to have been able to measure the cross-correlation interval for a smaller frequency separation. However, the 137/360 MHz data were the only available two frequency data.

8. Schwartz, M., Bennet, W. R., and Stein, S. (1966) Communication Systems and Techniques, McGraw-Hill.

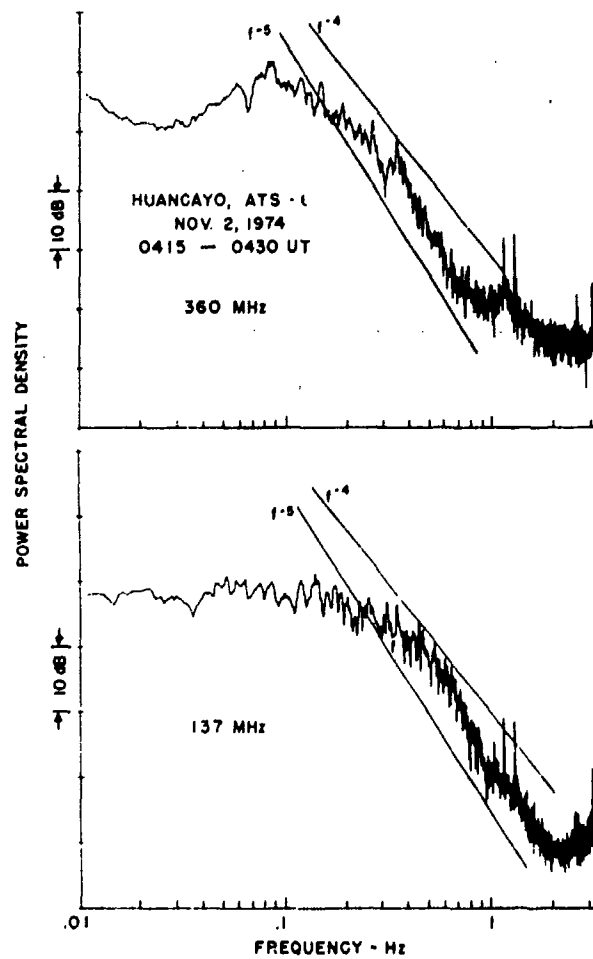
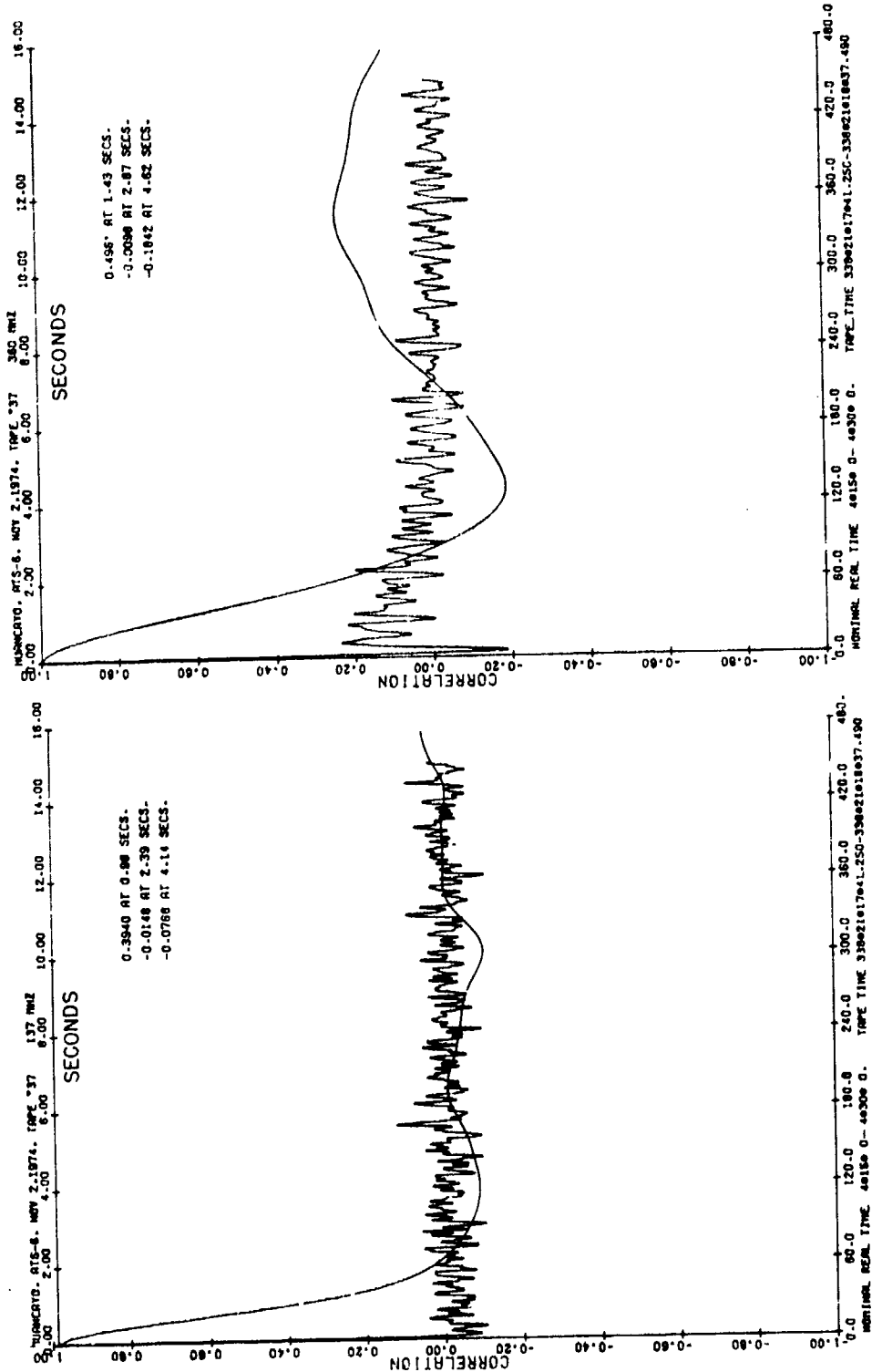


Figure 4. Typical Power Spectra for Intense Scintillations at 137 MHz and 360 MHz

Table 2. Summary of Data Reduction

DATA SET UT		cdf		AUTO-COR. INTERVAL $\rho = 0.5$		137 MHz POWER SPECTRA			360 MHz POWER SPECTRA			CUTOFF $\frac{x}{T}$		FREQ. DEP.	
START	END	m_{137}	m_{360}	τ_{137}	τ_{360}	SLOPE LOW	SLOPE HIGH	CUTOFF FREQ.	SLOPE LOW	SLOPE HIGH	CUTOFF FREQ.	K_{137}	K_{360}	η_m	
PERU 2 Nov. 1974															
0315	0330	1.32	3.93	.76	.90	1.91	5.35	.59		4.57		.45		1.13	
0330	0745	1.01	2.02	.55	.99	.43	5.95	.56	2.55	4.95	.33	.31	.33	.72	
0345	0400	1.09	1.89	.60	1.01	1.63	5.75	.59	3.05	4.90	.34	.35	.34	.45	
0400	0415	1.12	1.42	.60	1.25	1.63	5.88	.61	3.45	5.31	.37	.37	.46	.25	
0415	0439	1.14	1.64	.81	1.41	1.98	5.08	.47	2.55	7.25	.37	.38	.52	.38	
0430	0445	2.22	14.98	2.2	1.90		3.80			2.92				1.98	
0445	0500	7.72	59.7	2.65	1.90		3.63			2.29				2.12	
PERU 5 Nov. 1974															
0118	0148	1.21	1.48	.32	.76	.76	4.40	.90	.88	4.09	.36	.32	.27	.21	
0133	0303	1.15	1.82	.40	.75	.81	4.66	1.0	.88	4.21	.39	.4	.29	.48	
0148	0203	1.71	2.13	.39	.75	.60	3.98	.86	.88	4.26	.36	.34	.27	.24	
0203	0218	2.22	12.8	.97	1.05	.99	4.32	.32		3.41		.31		1.81	
0218	0233	1.84	7.46	.97	1.13	1.87	4.89	.46		3.88		.45		1.45	
0233	0248	1.33	4.65	.78	1.00	1.00	5.2	.47		3.81		.37		1.30	
0248	0303	1.16	3.43	.78	.81	.93	5.09	.48		3.67		.37		1.12	
0348	0403	1.27	3.08	1.11	1.75	1.19	6.57	.33		4.59		.37		.92	
0403	0418	1.47	5.22	1.62	2.30	1.22	4.86	.25		3.68		.41		1.31	
0418	0433	2.13	13.3	2.48	2.40		4.51			3.32				1.89	

DATA SET UT		cdf		AUTO-COR. INT. $\rho = 0.5$	POWER SPECTRA
START	END	m_{137}	τ_{137}		SLOPE
NARSSARSSUAQ 20 July 1974					
0500	0515	20.3	1.00		1.71
0515	0530	21.5	3.75		1.93
0530	0545	4.48	71.4		1.65
0545	0600	3.27	7.65		2.16
0600	0615	1.54	1.50		2.89
0615	0630	1.60	1.42		3.24
0630	0645	1.30	1.71		2.98
0645	0700	3.08	2.12		2.73
0700	0715	1.97	4.68		2.61
0715	0730	1.82	3.0		2.72
0730	0745	2.52	2.55		3.19
0745	0800	1.58	1.62		3.94
0800	0815	2.07	3.40		2.73
0815	0830	7.10	4.33		2.0



CORRELATION INTERVAL - τ (SECONDS)
 Figure 5. Typical Autocorrelation Functions for Intense Scintillations at 137 MHz and 360 MHz

3. RESULTS

Table 2 is a summary of the important statistics of the analysis of the 31 data samples. The table lists the Nakagami m-parameter; the correlation interval, τ , for an autocorrelation coefficient $\rho = 0.5$; the 'cut-off' frequency and the slopes of the power spectrum; the calculated value of the spectral index for samples having two frequencies; and the calculated value of the product of the 'cut-off' frequency and the correlation interval, τ .

The Nakagami m-parameter is related to the rms value of the intensity of the scintillations. It completely describes the distribution. Reference 4 has shown that the distribution function of ionospheric scintillations closely approximates the theoretical Nakagami distribution. While m can have any value ≥ 0.5 , all the data that has been analyzed indicates that $m = 1$ is the limiting case which corresponds to the Rayleigh distribution. The circles in Figure 1 are points for a Rayleigh distribution, ($m = 1$), and show the agreement of the 137 and 360 MHz data with the Nakagami distribution. The Chi-square test indicates that there is a better fit of the data to the Nakagami distribution than to the log-normal distribution. Figure 7 is a plot of the Nakagami distribution in cumulative form for several values of m. The experimental data indicates that the Rayleigh distribution or the $m = 1$ curve in Figure 7 is a limiting case for scintillations in the 200 to 400 MHz band. Figure 7 can therefore be used to estimate the expected fading under 'worst' case conditions for various percentiles.

Reference 4 has shown that the spectral index or frequency dependence of scintillations can be related to the m-parameter in the following way:

$$\eta_m = \frac{\log \frac{m_1}{m_2}}{\log \frac{r_1}{r_2}}$$

where η_m is the spectral index and m_1 and m_2 are the Nakagami values measured at the two frequencies, f . This assumes that the scintillation index or m remains a constant power of frequency over the measurement range. Table 2 lists the calculated values of the spectral index for the 17 sets of two frequency data and the distribution is plotted in Figure 8. While the scintillations at 360 MHz did not have the intensity to actually measure a value of $\eta_m = 0$, it is expected that this could be achieved as the 'worst' case condition. There were several measured values of η_m in the lowest range of 0.2 which indicates very little decrease of scintillation intensity with frequency. This is another indication that the 'worst' case fading in the 200 to 400 MHz band can be approximated by a Rayleigh distribution.

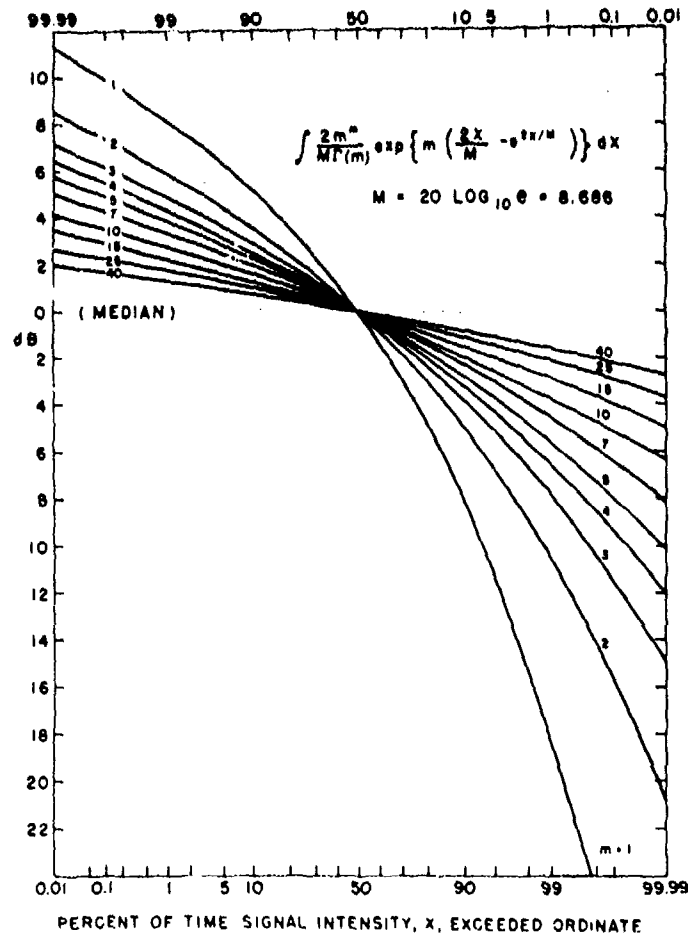


Figure 7. Cumulative Form of Nakagami m-Distribution; Valid for $m \geq 0.5$

In addition to the information on the depth of fading, information on the rate of fading is also required to fully understand the effects of scintillations on the communications channel. The statistics on the fading rates has been measured and presented in three ways; (1) the autocorrelation function, (2) the power spectrum, and (3) the tabulation of the results of the level crossing technique in the form of the duration of fades below and increases above given levels and message reliability. Since time diversity is effectively achieved in the application of coding techniques to the AFSATCOM system, it is felt that the autocorrelation information is the easiest to apply in evaluating the fade rate data.

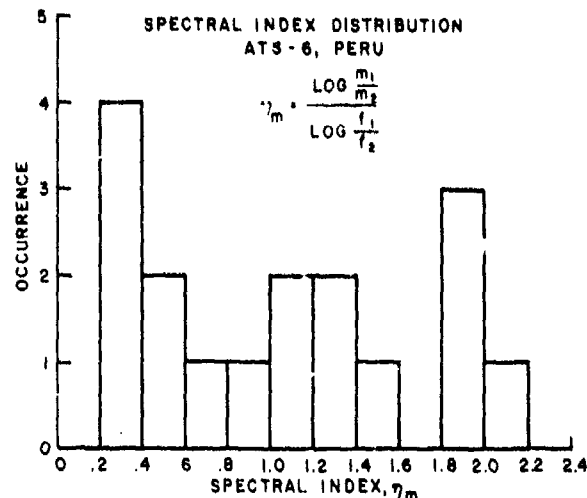


Figure 8. Occurrence of Spectral Index (η_m) Values From a Data Base of 17 Pair of 15-min Amplitude Distributions of 137 and 360 MHz Scintillations; m = Nakagami's Distribution Parameter

When correlation data is available it can be used to determine the improvement in performance that can be obtained through the application of diversity techniques. Auto-correlation data can be used to evaluate time diversity techniques; cross-correlation data from multifrequency measurements can be used to evaluate the effectiveness of frequency diversity; and, if spaced receiver measurements are available, then the cross-correlation information can evaluate space diversity. Figure 9 is adapted from Reference 8 and shows the improvement in performance that is possible with dual-diversity techniques. The probability of achieving diversity gain is given for several values of ρ , the correlation coefficient. It is based on slow, multiplicative Rayleigh fading and equal signal-to-noise ratios in both branches of a dual diversity system. Reference 8 used $|\rho|$, the magnitude of the complex cross-correlation, while Figure 9 uses the envelope cross-correlation. Most of the diversity improvement is achieved by the time $\rho = 0.6$. For example the improvement at the 1 percent point is approximately 8 dB for $\rho = 0.6$ and 10 dB for $\rho = 0$ or complete decorrelation.

The correlation intervals for $\rho = 0.5$ of the 17 sets of 137/360 MHz data are plotted in Figure 10 to show the relationship that holds for this very limited set of data. For small delays the 360 MHz value is approximately twice the 137 value. At longer delays the values tend to be the same.

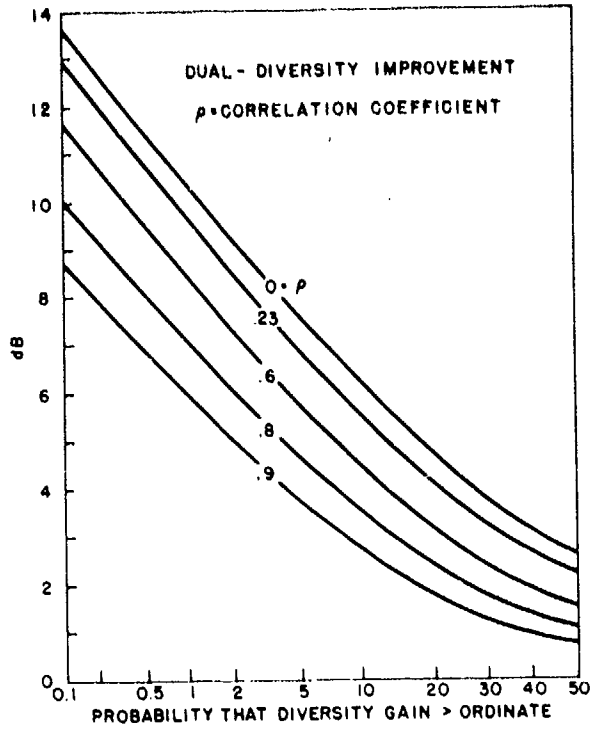


Figure 9. Improvement in Signal-to-Noise Ratio With Dual-Diversity Techniques Under Conditions of Rayleigh Fading

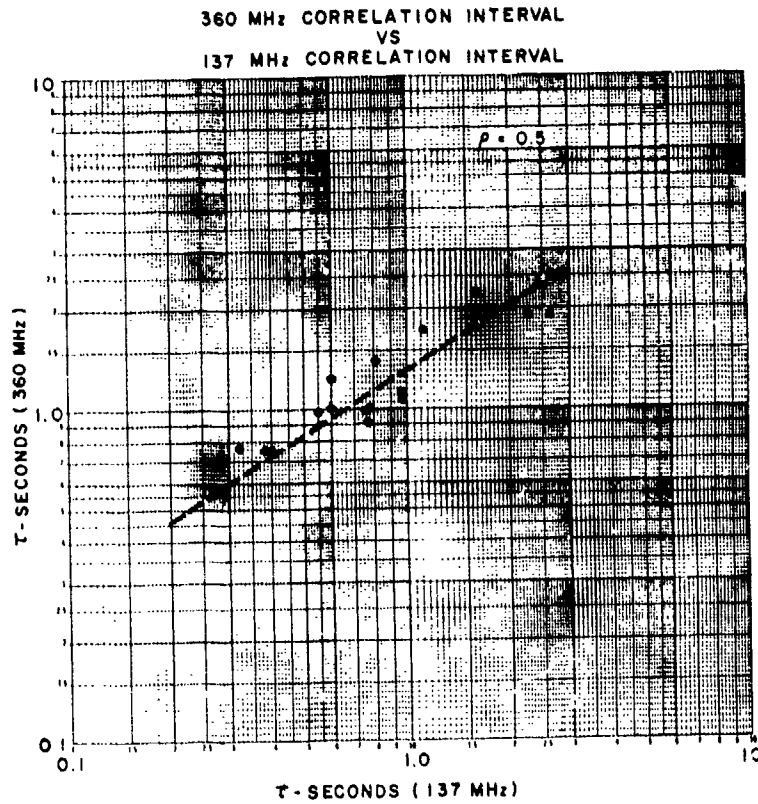


Figure 10. Variation of Autocorrelation Intervals for Two Frequency Data Samples

The variation of the correlation interval with intensity of scintillation is shown in Figure 11. The measured values at each frequency for the 17 sets of data are plotted against the Nakagami m-parameter which was measured from the corresponding cdf. An ellipse has been drawn to encompass the data at each frequency to give the apparent variation with m.

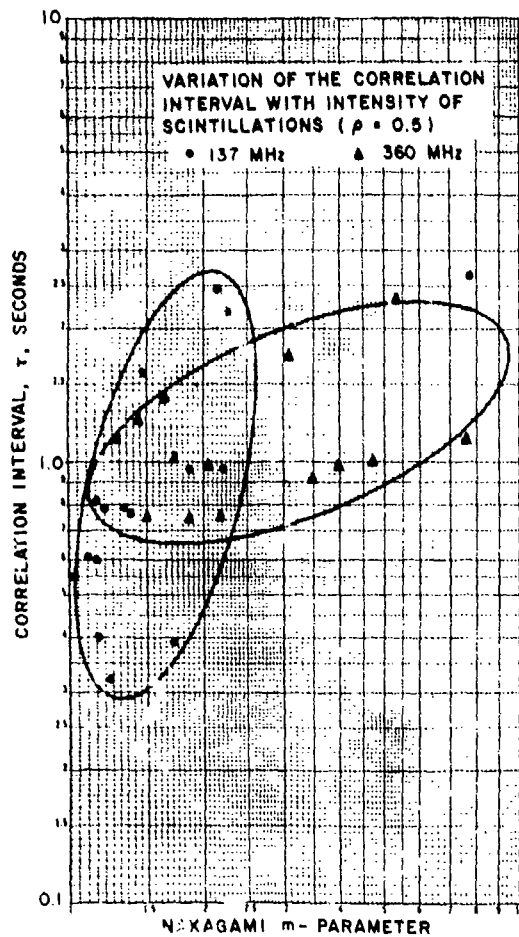


Figure 11. Variation of the Correlation Interval With Intensity of Scintillations for Two Frequency Data Samples

The values of the correlation interval for the Narssarssuaq data were generally greater than for the Peru data, even though they were both measured at the same frequency, 137 MHz. It is felt that this is not a difference between the equatorial and auroral regions but rather it is caused by the Narssarssuaq data having less intensity of scintillations than the Peru data.

For those periods given in Table 2 for which a cutoff frequency could be measured in the power spectrum, a constant was calculated from the product of the cutoff frequency and the autocorrelation interval, τ . The values are tabulated in Table 2 under the heading K_{137} and K_{360} . The averages of the measurements for both frequencies were almost equal, $K_{137} = .37$ and $K_{360} = .35$.

4. CONCLUSIONS AND RECOMMENDATIONS

From a large collection of observations a limited amount of VHF/UHF data has been analyzed to determine the amplitude and rate characteristics of intense scintillations. The results are in the form of amplitude distributions, level crossing tabulations, power spectra and correlation data. While a Rayleigh distribution was not exactly measured, it was judged that this would be the limiting case up to at least 400 MHz. This is in agreement with the spectral index data which indicated that fading of the most intense samples was almost independent of frequency. The autocorrelation and power spectra data defined the fading rates and provided a base for the evaluation of time diversity techniques. Only three samples of cross-correlation (137/360 MHz) were processed and coefficients less than 0.4 were obtained. However, this frequency separation was really too great to determine the applicability of frequency diversity techniques within the bandwidth normally available to satellite communication systems.

Much remains to be done to characterize the intense scintillations that are observed in the equatorial region. Multifrequency observations are necessary to determine the frequency dependence and the evaluation of diversity techniques in the UHF range.

References

1. Aarons, J., Whitney, H. E., and Allen, R. S. (1971) Global morphology of ionospheric scintillations, Proc. IEEE 59:159.
2. Crane, R. K. (1974) Morphology of Ionospheric Scintillation, Technical Note. Lincoln Laboratory, 1974-29, Air Force Contract F19628-73-C-0002.
3. Aarons, J. (1975) Global Morphology of Ionospheric Scintillations II, AFCRL-TR-75-0135.
4. Whitney, H. E., Aarons, J., Allen, R. S., and Seemann, D. R. (1972) Estimation of the cumulative amplitude probability distribution function of ionospheric scintillations, Radio Science, 7, No. 12:1095-1104.
5. Briggs, B. H., and Parkin, I. A. (1963) On the variation of radio star and satellite scintillations with zenith angle, J. Atmos. Terr. Phy., 25:330-366.
6. Nakagami, M. (1960) Statistical methods, in Radio Wave Propagation, edited by W. C. Hoffman, pp. 3-36, Pergamon, New York
7. Christopher, P. (1975) Moments of a Log-Nakagami Distribution and Application, Mitre Corporation Memo D91-M-4024.
8. Schwartz, M., Bennet, W. R., and Stein, S. (1966) Communication Systems and Techniques, McGraw-Hill.